

# Polyaniline as a Hippocampus-inspired Biomimetic Device for Electrochemical Monitoring of Phosphorylated Tau induced Neurodegenerative Processes

**Chien-Chih Hsu**

National Chiao Tung University

**Yu-Rong Wang**

National Chiao Tung University

**Adarsh Tripathi**

National Tsing Hua University

**Yu-Lin Wang**

National Tsing Hua University

**Jung-Chih Chen** (✉ [george@nctu.edu.tw](mailto:george@nctu.edu.tw))

National Chiao Tung University <https://orcid.org/0000-0003-3958-6806>

---

## Research Article

**Keywords:** Phosphorylated tau, Electrochemistry, Dephosphorylation, Quartz crystal microbalance (QCM), Alzheimer's disease (AD)

**Posted Date:** April 8th, 2021

**DOI:** <https://doi.org/10.21203/rs.3.rs-377393/v1>

**License:**  This work is licensed under a Creative Commons Attribution 4.0 International License.

[Read Full License](#)

---

# Abstract

Tau protein plays an important role in Alzheimer's Disease (AD), especially its hyper-phosphorylated state, which is involved in aggregating and triggering entangled nerve fibers, eventually leading to neuronal death. This study investigates whether this hyper-phosphorylated tau can be dephosphorylated by electrochemical techniques. Aiming at the phosphorylation sites only found in AD brain, we utilized human tau (pS214) peptide as the target for this study. With the help of electrochemical quartz crystal microbalance (EQCM) system, we utilized electrochemical methods to trigger interaction between potential charge and tau protein and monitor the whole reaction on the electrode by QCM. The polyaniline membrane was then used as a hippocampus-inspired biomimetic device to observe charge-protein interactions where positive potential attaches phosphorylated tau and negative potential detaches the phosphoryl group. We successfully found out that 0.5 V can induce complete attachment to phosphorylated tau and - 0.3 V can achieve dephosphorylation of tau peptide. Furthermore, to demonstrate dephosphorylation of tau peptide, we performed mass spectrometry to examine the reaction product and prove our hypothesis. To sum up, this device could be a potential novel treatment for tau-related neurodegenerative diseases.

## Introduction

Alzheimer's disease (AD) has been the most common cause of dementia for several years [1]. There are two major causes of the disease. One is the accumulation of  $\beta$ -amyloid around the cerebral cortex to form plaques and the other is tau protein hyperphosphorylation, triggering tau aggregation and nerve fibers entanglement, leading to neuronal death [2–4]. These pathological features have caught everyone's attention on AD research for decades [5, 6]. In recent studies,  $\beta$ -amyloid became a good target for early detection and tau seem to be targeted more for its potential to develop treatment [7].

In the past decade, pharmaceutical companies, researchers, and the biotechnology industry have actively sought solutions to Alzheimer's disease and synthesized more than one hundred new drugs to fight dementia, but the developed drugs were not very effective and had many drawbacks [8, 9]. Most of the new AD drugs developed by the pharmaceutical companies failed in the second and third clinical trials, because of their side effects and no significant improvements on patient health [10–12]. Thus, non-drug treatment seems to be an alternate trend in AD remedy development.

As a marker of AD, tau protein has become an ideal target for treatment development [13]. The formation of neurofibrillary tangles (NFTs) is composed of abnormally modified tau, which is also known as hyper-phosphorylated tau [14]. The largest tau isoform (Tau441), contains 85 phosphorylation sites. Among these, 28 sites are specifically found in AD brains [15]. Research on dephosphorylation of these sites is expected to yield promising results in the treatment of Alzheimer's disease [15, 16].

Polyaniline (PANI) is a good conducting polymer to be used as protein carrier and it is widely used in electrochemical research and development [17–20]. Recently, it has been used in catheters to stimulate

nerve growth and recovery of functional neurons[21, 22]. Hippocampus is the part of the brain that controls short-term memory and the first area to shrink in the brain of AD patients [23, 24]. Utilizing these two concepts, it is hypothesized that polyaniline could be used in hippocampal gyrus nerve regeneration and repair in the future [25]. Our study explores the possibility of treating polyaniline as a hippocampal gyrus analog to simulate phosphorylated tau protein attachment and also the removal of phosphate groups, similar to observing these effect on nerves.

Thus, our research adheres to the goal of developing a tool for treating Alzheimer's disease, using conductive polymer polyaniline as hippocampal gyrus analog, and electrochemical methods combined with quartz crystal microbalance as an observation platform to explore the feasibility of changing potential to stimulate dephosphorylation on tau protein. Overall, this study is thought to establish a milestone towards treatment of tau induced neurodegenerative disease.

## Materials And Methods

### Chemicals

Human tau phosphor S214 peptide was purchased from Abcam (Bristol, UK). Phosphate-buffered saline (PBS) (10X, pH 7.4) was obtained from Thermo Fisher Scientific Inc (Waltham, MA, USA). Aniline (99.5%), potassium hexacyanoferrate (II), potassium hexacyanoferrate (III), potassium chloride (KCl), and sulfuric acid were purchased from Sigma-Aldrich (St. Louis, MO, USA). All chemicals were of analytical grade and used without further purification. All aqueous solutions were prepared with double deionized water (18 MΩ cm, Merck Millipore, USA)

### Electrochemical methods

EQCM system was supplied in a three-electrode setup from CH instruments, USA, Model CHI-405C (Fig. 1). Three electrochemical methods were utilized in our study, including chronoamperometry, cyclic voltammetry, and amperometry. Chronoamperometry (CA) was used to generate polyaniline membrane on electrode as hippocampus-inspired biomimetic device. The potentials were set at 0.8 V and 0.5 V, and simulate each potential 8 times in 20 seconds for a cycle, totally simulate 16 cycles. Cyclic voltammetry (CV) was performed in 5 mM  $K_4Fe(CN)_6 / K_3Fe(CN)_6$  (1:1 ratio) in 1 M KCl for the electrode conductivity test. The potential was provided between +0.1 V to +0.5 V at  $10 \text{ mV s}^{-1}$ . Amperometry was used with fixed potential to test different potentials which attach to phosphorylated tau and cause dephosphorylation effect.

### Quartz crystal microbalance

Quartz Crystal Microbalance (QCM) is an extremely sensitive mass measurement tool that can measure the mass change ranging from nanograms to micrograms. The main body is a thin quartz crystal

sandwiched between two metal electrodes. By forming an alternating electric field across the entire crystal, the crystal vibrates at its own resonance frequency. At the same time, vibration frequency is affected by the mass changes of the crystal and electrodes. Monitoring this frequency change in real time, and then transferring the signal process to the corresponding software, signal output is generated and digitized. We used this method in the all electrochemical experiments that can perform real-time monitoring of changes on electrode surface.

## HPLC/ESI-MS/MS

Mass Spectrometry (MS) is a technique used to analyze molecular mass of a peptide sequence. After analyte molecules are converted into ions, they are separated according to their mass-to-charge ratio ( $m/z$ ), which can provide qualitative (e.g. structure) and quantitative information (e.g. molecular mass, concentration) of the target protein. In our study, Electro Spray Ionization-Mass Spectroscopy (ESI-MS) was used to detect the substrate removal from the electrode, ensuring that the dephosphorylation of tau peptide was successful. Stock solution was used as standard for the target from HPLC-ESI-MS results. After phosphor S214 tau peptide was attaching on the electrode, the solution was examined for protein as negative control. Tau protein content in standard solution and experimental sample were then compared in order to know the exact progress by the reaction.

## Results

### Electrochemical synthesis polyaniline membrane

The polyaniline film was constructed as described in Section 2.2 after the gold electrode was cleaned with nitrogen. The result of film formation in our study was achieved using chronoamperometry method. Two potentials, 0.5 V and 0.8 V, were used for 20 seconds each. Each of the potential was stimulated for 8 times, for a total of 16 cycles, and the time setting was decided by the amperometry method which was tested before with ideal thickness. The average time of synthesis by amperometry method was 160 seconds. We doubled the overall film forming time to last for 320 seconds.

The current graph shows that a pulse current would be generated at the exactly the time of potential switch. Fig. 2a shows that the potential rise would generate a positive current, and the potential drop generates a negative current. The current intensity increased with polyaniline film formation and gradually increased to 0.01 A, which was constant from that time onwards, meaning that the film formed has good conductivity and sustainability. It can be seen in the Fig. 2b that the frequency dropped sharply at 0.8 V, while the frequency dropped at relatively slower rate at 0.5 V, appearing in a ladder shaped drop on the delta frequency graph . After forming the polyaniline film, cyclic voltammetry was used to check its conductivity.

The polyaniline film was formed as shown in Fig. 2c. Electrode surface was green in color, and appeared as a thin green membrane visible with naked eyes. After PANI film was formed on the electrode, cyclic

voltammetry was used to confirm the conductivity. Fig. 2d shows that the polymer conductivity performed very well. Comparing this film with bare gold electrode and PANI generated by other method (Fig. 2e), it could be inferred that our PANI film had higher current conductivity than bare gold electrode and more stable current with negligible shift as compared to other method. This shows that using chronoamperometry to generate PANI films had good conductivity and stability, which is good enough to be used as a hippocampus gyrus biomimetic device.

## Positive potential attach p-tau

In addition to the fact that proteins are generally negatively charged, phosphorylated tau are more negatively charged [26, 27]. In this part, we used positive potential as an auxiliary tool for p-tau adsorption, and compared with other proteins for natural deposition on the membrane. An additional positive potential stimulation was provided to observe whether the adsorption could be enhanced, and hence, to prove that positive potential stimulation can induce the adsorption of phosphorylated tau.

Cyclic voltammetry can be used as a preliminary test for potential adsorption of proteins [28, 29]. Therefore, we first added 1  $\mu\text{l}$  of phosphorylated Tau (1 mg / ml) to the electrolytic cell and dissolved in 3 ml of ultrapure water and used cyclic voltammetry to sweep the positive potential range. These results and oxidation and reduction peak potentials generated from the solution mentioned before could be used together to establish a preliminary qualitative data for adsorption. As shown in Fig. 3a, after cyclic voltammetry sweeps the positive potential ranges from 0.1 V to 0.8 V going back and forth in this range. The range between 0.3 V to 0.6 V seem to be a potential selection choice. The current oxidation peak was between 0.5 V and 0.6 V, and there was a downward trend in the sweep from 0.6 V to 0.3 V during frequency change. So, the positive potential range was restricted from 0.3 V to 0.6 V, and this result was used to do further fixed potential adsorption tests.

After the PANI membrane was formed, four potentials were selected for fixed potential to be used for adsorbing phosphorylated Tau test. In addition, natural deposition without any additional potentials provided was included for comparison. The frequency decrease amplitude generated by different electric potentials is shown in Fig. 3b. 0.5 V adsorption effect was proven to show the highest change where the frequency dropped by 285 Hz, and the mass change per unit area of the electrode surface was about 1.95  $\mu\text{g}/\text{cm}^2$ . 0.3 V potential showed the second highest change, where the frequency dropped by approximately 135 Hz. This change could be calculated into a mass of approximately 0.92  $\mu\text{g}/\text{cm}^2$  on the electrode surface. These results showed that these two fixed potentials were good for adsorption of phosphorylated Tau. 0.5 V was then used as the primary fixed potential for further experimentation because of its higher drop.

Based on the results of the previous part of the experiment, phosphorylated Tau adsorption due to positive potential was reproduced using 0.5 V fixed potential. After the PANI film was formed and checked for conductivity, the adsorption confirmation test was performed using low-concentration phosphorylated

Tau (0.33  $\mu\text{g}/\text{ml}$ ), high-concentration phosphorylated Tau (1  $\mu\text{g}/\text{ml}$ ), and ultrapure water. These tests were performed in triplicates and averaged for comparison, and results are shown in Fig. 3c. When using ultrapure water, the frequency drop averaged at 38 Hz, which was converted into a mass change per unit area of about 0.26  $\mu\text{g}/\text{cm}^2$ . When using a low concentration phosphorylated Tau solution for adsorption, the average frequency drop was 283 Hz, which was converted to the mass change per unit area of about 1.93  $\mu\text{g}/\text{cm}^2$ . However, for the high concentration phosphorylated Tau, the average frequency drop was about 933 Hz, which was converted into the mass change per unit area of about 6.38  $\mu\text{g}/\text{cm}^2$ . As a result, it can be confirmed that 0.5 V seems to be the most ideal potential to be used to attach phosphorylated tau to PANI membrane, as compared to other fixed potentials, and using 0.5 V as fixed potential can certainly achieve adsorption of specific-site phosphorylated tau.

## Negative potential removes p-tau and achieve dephosphorylation

In this part, we first used 3 ml of low-concentration phosphorylated Tau (0.33  $\mu\text{g}/\text{ml}$ ) for adsorption and desorption tests. Cyclic voltammetry was applied by screening at different voltages, Fig. 4a shows that -0.3 V ~ -0.5 V has a trend of dephosphorylation in frequency change and charge effect. Thus, we applied -0.3 V, -0.4 V, and -0.5 V as fixed negative potential to test if dephosphorylation can be achieved.

After positive potential was stimulated to adsorb phosphorylated Tau on the PANI membrane, the frequency change caused by adsorption was found to be at 350 Hz, and repulsion test was performed by three negative potentials as mentioned before (Fig. 4b). In the test involving low-concentration phosphorylated Tau, the frequency change of -0.3 V has a small change of about 450 Hz is detached, which is converted to mass per unit area of about 3.08  $\mu\text{g}/\text{cm}^2$ . -0.5 V has the best detach effect. After the drive is detach, the frequency increases to 800 Hz, which is converted to a mass per unit area of about 5.47  $\mu\text{g}/\text{cm}^2$ . These results can confirm that all three potentials have repulsion effects. Among them, -0.3 V is closest to phosphate repelling potential that this study is aiming for. The concentration is increased for further testing.

In the high-concentration phosphorylated Tau test, the concentration of phosphorylated Tau was increased where 1  $\mu\text{g}/\text{ml}$  of the protein was added to 3 ml of the solution and put into the device, and controlled by 0.5 V positive potential. the adsorption of phosphorylated Tau can achieve a frequency change of 1000 Hz. Identical adsorption amount was used to carry out -0.3, -0.4 V and -0.5 V fixed potential dephosphorylation tests. The results are shown in Fig. 4b. The effect of negative potential to remove phosphorylated Tau increased the most at -0.5 V, followed by -0.4 V. Frequency change at -0.3 V increased by 700 Hz, which was converted to mass per unit area for the removed p-Tau at 4.78  $\mu\text{g}/\text{cm}^2$ . The results were similar to those when lower concentration phosphorylated Tau were used. Compared to the other two negative potentials, -0.3 V was less effective in removing phosphorylated Tau. It also shows the ability to remove a certain quantity of proteins. However, the main point of this research is to find a

negative potential that can remove phosphate, rather than the entire tau. With reference to the peak position of the cyclic voltammetry current in the previous part, it is suspected that the possible potential of dephosphorylation is -0.3 V.

Finally, in order to ensure the desorption effect and reproducibility of -0.3 V, and to confirm that the repelled protein is phosphorylated Tau or phosphoryl group, in this part, we carry out three repetitive experiments. After the PANI film was formed, 0.5 V was used as adsorption potential, and then removal by -0.3 V potential. The result can be seen in Fig. 4c. During adsorption, the phosphorylated Tau was adsorbed at a fixed potential of 0.5 V and decreased at an average frequency of 933 Hz, which was converted into a mass change per unit area of approximately  $6.38 \mu\text{g}/\text{cm}^2$ . During repulsion, phosphorylated Tau or only phosphate group was removed by -0.3 V and produced an average frequency increase of 793 Hz, which is converted into a mass change per unit area of approximately  $5.42 \mu\text{g}/\text{cm}^2$ . Compared with the standard deviation of the adsorption frequency, the frequency of the repulsion was relatively stable. This is considered to be affected by the hydrogen ion interference, but the overall performance was still stable and reproducible.

## Mass spectrometry to examine the solution

After the successful repulsion test at negative potential of -0.3 V, the frequency change measured by quartz crystal microbalance showed that the material on the electrode can be driven into the solution at this negative potential. However, it cannot be ensured if the corresponding substance is phosphate or the entire phosphorylated Tau. Therefore, to investigate the repelled substance, in this part of study, the solution containing of the repelled substance was detected by high performance liquid chromatography mass spectrometer (HPLC-MS).

First, in order to determine the mass-to-charge ratio and molecular weight of phosphorylated Tau used in this study, stock solution purchased from the manufacturer was analyzed using HPLC-MS. As shown in Fig. 5a, the target peptide was separated by HPLC. After being extracted, the molecules were ionized by the ion source of mass spectrometer, and the mass analyzer separates them according to their mass-to-charge ratio to produce results. Fig. 5a shows that there are three sharp peaks, namely 562, 702 and 936. After deconvolution and back-calculation, it can be seen that these three peaks correspond to p-tau peptides used in the experiment. The  $m/z$  size was about 2806, and the signal strength was  $2.5 \times 10^6$ , with the detection limit of about 0.6~0.3 ppm.

In this study, in order to minimize error and to eliminate interference, deionized water which was used for solution preparation in experiments was also tested by mass spectrometer as a negative control group with no Tau added to it and the result can be seen in Fig. 5b-l. The largest signal is obtained at 705, a peak with an intensity of  $1.6 \times 10^4$ . However, in terms of mass spectrometer results, this signal is too small and can be neglected. In the previous part of the standard, there was no obvious signal generated at the three peak positions. It proves that negative control does not contain any substance that may

interfere with the experiment, and subsequent experiments would be able to compare and confirm phosphorylated Tau with the three peaks measured by standard mass spectrometer.

In order to confirm that the phosphorylated Tau is adsorbed on the polyaniline film electrode, this part operated an additional mass spectrometry test on the waste liquid after the adsorption was completed with a positive potential of 0.5 V in the experiment to check whether the solution still contained any phosphorylated Tau or not, and the result is as shown in Fig. 5b-II. As compared to the standard product in Fig. 5a, there was no obvious phosphorylated Tau peak in the solution, and the dominant signal was the impurity peak. This can help prove that most of the phosphorylated Tau added to the solution was adsorbed. So the signal value of phosphorylated Tau cannot be detected in the solution.

The sample composition for the third part of this experiment is as shown in Supplementary Figure 1. The solution containing the substance removed by negative potential -0.3 V was used as the experimental target, and the phosphorylated Tau stock solution was diluted as the control group. Results are as shown in Fig. 5c, in both experimental group and control group, there was a main peak of 936. The signal intensity of the control group was  $3.8 \times 10^5$ , and the signal intensity of the experimental group was  $1 \times 10^5$ . The difference was about four times between the two samples, and this peak was identical to the trivalent peak results in Fig. 5a. Therefore, it can be confirmed that this peak represents phosphorylated Tau. It also showed that the positive adsorption potential and negative potential used in this study remove phosphorylated Tau were true, and the phosphorylated state can be measured using a mass spectrometer.

Beside the phosphorylated Tau signal, there are two obvious peaks at m/z 861 and 839. According to prior studies [30, 31], these two peaks can be presumed as unphosphorylated and dephosphorylated Tau respectively. After rearrangement, the results shown in Table 1 display these three peaks by their intensity and percentage. Using the overall Tau percentage, it can be found that the ratios of phosphorylated Tau detected by mass spectrometer in the two groups are similar, while the ratio of dephosphorylated Tau in the experimental group is much higher than that in the control group. The ratio of unphosphorylated Tau is relatively small. It is noteworthy that the unphosphorylated Tau of the control group is about 11 times as compared to the experimental group, while the dephosphorylated Tau of the control group is double as compared to the experimental group. The dephosphorylated Tau in the experimental group has been greatly increased, which proves that -0.3 V potential used in this study not only removes the phosphorylated Tau, but also achieves the dephosphorylation effect. This part also confirms that the 0.5 V positive potential used in this study also has the effect of adsorbing phosphorylated Tau on PANI surface, and when -0.3 V negative potential was used, it not only drove away phosphorylated Tau, but also dephosphorylated phosphorylated Tau peptide.

Table 1

Comparison of control and experimental mass spectrometry results. Phosphorylated tau, unphosphorylated tau and dephosphorylated tau intensity and ratio are compared

Peak	Meaning	Control		Experimental	
		Intensity	Percentage	Intensity	Percentage
936	$[M+3H]^{3+}$	$3.8 \times 10^5$	52%	$1 \times 10^5$	58%
861	$[M+3H]^{3+} - PO_3^{2-}$	$2.5 \times 10^5$	34%	$0.2 \times 10^5$	12%
839	$[M+3H]^{3+} - H_3PO_4$	$1 \times 10^5$	13%	$0.5 \times 10^5$	29%
* "-" means a minus sign here					
* % (Percentage) is calculated by the signal intensity ratio of the three peaks					

## Discussion

In this study, an electrochemical platform was used to simulate the pathogenesis of tau protein in the brain of AD patients, including phosphorylated tau aggregation and dephosphorylation tests. Polyaniline polymer film was used as a hippocampus gyrus mimic. The standard parameters and conditions of electrochemical methods were successfully established to make the PANI film preparation reproducible. PANI film was formed as a protein carrier, with good conductivity and stability. The properties and the establishment of successful film forming conditions make the film forming time longer and allow it to become a more stable structure.

As the memory center of the brain, hippocampus is the first area in the brain of AD patients that begins to shrink, playing an important role in many AD studies [32, 33]. Additionally, hippocampal gyrus is the earliest site of nerve fiber entanglement caused due to the hyperphosphorylation of tau protein [34], which makes dephosphorylation of tau more important as research target. For the choice of hippocampal gyrus mimics, as mentioned in previous section, PANI has good electrical conductivity and biocompatibility, and to some degree, they have many biologically relevant similarities. Therefore, it is suitable to be used to simulate the adsorption and dephosphorylation effects of phosphorylated Tau as a hippocampus mimic.

In the current electrochemical analysis of phosphorylated proteins, electrodes are mainly used for monitoring phosphorylation process. Specific phosphorylated proteins were captured by immunosensors and antibodies, and then detected using electrochemical impedance method. In order to detect phosphorylated proteins, electrode can also be used as a phosphorylation tool [35, 36]. After adsorbing the protein, the protein is phosphorylated through an enzymatic reaction, electrochemical impedance analysis and other methods are used to achieve protein concentration estimation and other applications related to phosphorylation of tau protein [37]. In addition, there are studies combining phosphokinase with electrodes to phosphorylate proteins through enzyme biosensors [38], and electrochemically drive the phosphorylation of organic molecules [39]. Therefore, electrochemical applications of phosphorylated proteins are quite diverse. Our study expects to achieve the dephosphorylation effect of phosphorylated

peptides with slight changes in potential, and real-time monitoring of effect analysis by combining them with a quartz crystal microbalance.

The electrochemical research of tau protein is mainly focused on detection, i.e., the detection target for AD [40, 41]. On the other hand, there are some studies on the electrochemical real-time monitoring of the phosphorylation process of tau protein. One of the studies used the electrochemical impedance method to monitor the entire phosphorylation process, from the adsorption of tau on the electrode to the phosphorylation reaction using phosphokinase and adenosine triphosphate [42]. As the enzyme kinetic was analyzed by different concentrations of phosphokinase and adenosine triphosphate, a square wave voltammetry current signal and electrochemical impedance method were used to monitor and simulate the phosphorylation cascade reactions to study the continuous phosphorylation process of tau protein [43].

Our study intends to use positive potential stimulation to trigger the adsorption of specific-site phosphorylated tau, on the hippocampal gyrus, and to subsequently trigger dephosphorylation effect with negative potential. The reason why fixed potential is mainly used in this study is that it can achieve adsorption effect more stably. Compared with the protein adsorption without additional application of potential or the application of variable potential, the adsorption frequency change of fixed potential shows a relatively stable decline, and in some other studies, also utilize fixed potential as a protein adsorption method [44]. Therefore, our study used cyclic voltammetry method to screen through the front-end potential and use different fixed potentials to test which could better stimulate adsorption. The adsorption effect test was carried out to find an optimal adsorption potential which was found to be 0.5 V for phosphorylated Tau. This potential was then used as an auxiliary to facilitate the adsorption of different concentrations of phosphorylated Tau for confirmation experiments.

According to the forward results, the positive potential electrode can indeed achieve the effect of adsorbing phosphorylated Tau peptides. In this study, a variety of electrochemical methods were combined to determine the best adsorption potential. The adsorption effect was then observed at a fixed potential ranging between 0.3 ~ 0.6 V. An electrochemically combined quartz crystal microbalance system was used to achieve real-time observation of frequency and quality changes on the membrane. At the same time, high and low concentrations of phosphorylated Tau were tested respectively. The results showed that 0.5 V was the best adsorption potential for phosphorylated Tau protein. Appropriately, the since the adsorption effect for phosphorylated Tau is highest, it can show reproducibility and consistency. Therefore, it may be possible to use this positive potential as a strategy for adsorbing phosphorylated Tau proteins in the future. This method can also be considered to be used for further testing in biological experiments. Using this method, hyperphosphorylated Tau could be eliminated, and when applied to the brain of patients with Alzheimer's disease, it could potentially slow down the disease process.

In the low concentration tests, the frequency change after negative potential release is higher than the adsorption frequency, which is mainly due to the fact that the PANI film used in this study has good

conductivity, and the hydrogen ions would be repelled by the positive potential during positive potential adsorption. The removal would make the decreasing frequency reduced, compared to the actual adsorption, but the removed subunit would not be affected by this. Instead, it would be catalyzed by the negative potential to generate gas, which would increase the frequency even further [45], thus causing the frequency change higher than the adsorption frequency. When the concentration of phosphorylated tau increases to make the frequency change more significant, this problem could be eliminated [46].

Finally, the purpose of this study is to remove phosphate on phosphorylated Tau with negative potential. Cyclic voltammetry was used to perform potential screening, and a fixed potential ranging from -0.3 to -0.5 V was then used to monitor the repelling effect. In terms of potential selection, complete Tau protein was not used. Abandoning the result that the peptides are all driven away, therefore, the partial repellent potential of -0.3 V was selected. These results showed that the negative potential can successfully achieve partial repelling effect. Mass spectrometry is used to detect the solution of the repelled subunits. Solution was successfully detected using phosphorylated Tau peptides and change in the ratio of Tau peptides after dephosphorylation. Confirming that this negative potential has a dephosphorylation effect, it is expected to achieve the effect of removing phosphate group on the Tau peptide with negative potential, which is beneficial for future research in AD treatment.

## Conclusions

The recent emerging treatments for Alzheimer's disease are no longer limited to drug treatments, and non-drug treatment methods are booming. Our study focuses on real-time electrochemical monitoring of different potential changes for adsorption and dephosphorylation of specific site- phosphorylated tau peptides. Phosphorylated tau peptide effect, which is the main cause of Alzheimer's disease, can be dephosphorylated by using fixed potential method, which can be combined with transcranial magnetic stimulation and other electrical signal-related treatments in the future. In summary, our study successfully used 0.5V to attach phosphorylated tau and -0.3V to remove tau and dephosphorylate at the same time. This device could be a potential novel treatment in the field of tau-related neurodegenerative diseases. With appropriate application, our findings can become a complete treatment for AD patients.

## Declarations

## Acknowledgements

The authors appreciate the funding from the Ministry of Science & Technology and National Chiao Tung University. Also, thanks to the Precious Instrument Center and all colleagues in the laboratory who have assisted this research.

## Funding

This work was partially supported by research grants from Ministry of Science & Technology (MOST 108-2221-E-009-085) and National Chiao Tung University (109W153).

## Author Contributions

Methodology and writing original draft, Chien-Chih Hsu. Validation and writing editing, Yu-Rong Wang. Writing review, Adarsh Tripath. Supervision, Yu-Lin Wang. Resource, conceptualization and supervision, Jung-Chin Chen.

## Ethics declarations

Compliance with ethical standards

All research presented follows ethical standards.

## Conflicting Interests

The authors declare no competing interests.

## Consent to Participate

Not applicable

## Consent for Publication

All authors consent for the publication.

## Availability of Data and Materials

Not applicable.

## References

1. Laurent, C.L. BueeD. Blum, *Tau and neuroinflammation: What impact for Alzheimer's Disease and Tauopathies?* Biomedical Journal, 2018. **41**(1): p. 21-33.
2. Moreno-Jimenez, E.P.M. Flor-GarciaJ. Terreros-RoncalA. RabanoF. CafiniN. Pallas-BazarraJ. AvilaM. Llorens-Martin, *Adult hippocampal neurogenesis is abundant in neurologically healthy subjects and drops sharply in patients with Alzheimer's disease.* Nature Medicine, 2019. **25**(4): p. 554-560.

3. Mathys, H.J. Davila-Velderrain Z. Peng F. Gao S. Mohammadi J.Z. Young M. Menon L. He F. Abdurrob X. Jiang A.J. Martorell R.M. Ransohoff B.P. Hafler D.A. Bennett M. Kellis L.H. Tsai, *Single-cell transcriptomic analysis of Alzheimer's disease*. Nature, 2019. **570**: p. 332-337.
4. Ittner, A.L.M. Ittner, *Dendritic Tau in Alzheimer's Disease*. Neuron, 2018. **99**(1): p. 13-27.
5. Kim, B.S.E. Elzinga R.E. Henn L.M. McGinley E.L. Feldman, *The effects of insulin and insulin-like growth factor I on amyloid precursor protein phosphorylation in in vitro and in vivo models of Alzheimer's disease*. Neurobiology of Disease, 2019. **132**: p. 104541.
6. Panza, F.M. Lozupone G. Logroscino B.P. Imbimbo, *A critical appraisal of amyloid-beta-targeting therapies for Alzheimer disease*. Nature Reviews Neurology, 2019. **15**(2): p. 73-88.
7. Congdon, E.E.E.M. Sigurdsson, *Tau-targeting therapies for Alzheimer disease*. Nat Rev Neurol, 2018. **14**(7): p. 399-415.
8. Cummings, J.L.T. Morstorf K.J.A.s.r. Zhongtherapy, *Alzheimer's disease drug-development pipeline: few candidates, frequent failures*. 2014. **6**(4): p. 1-7.
9. Antolin, A.A.M. Ameratunga U. Banerji P.A. Clarke P. Workman B.J.S.r. Al-Lazikani, *The kinase polypharmacology landscape of clinical PARP inhibitors*. 2020. **10**(1): p. 1-14.
10. Yang, T.Y. Dang B. Ostaszewski D. Mengel V. Steffen C. Rabe T. Bittner D.M. Walsh D.J. Selkoe, *Target engagement in an Alzheimer trial: Crenezumab lowers amyloid beta oligomers in cerebrospinal fluid*. Annals of Neurology, 2019. **86**(2): p. 215-224.
11. Selkoe, D.J., *Alzheimer disease and aducanumab: adjusting our approach*. Nature Reviews Neurology, 2019. **15**(7): p. 365-366.
12. Moussa-Pacha, N.M.S.M. Abdin H.A. Omar H. Alniss T.H. Al-Tel, *BACE1 inhibitors: Current status and future directions in treating Alzheimer's disease*. Medicinal Research Reviews, 2020. **40**(1): p. 339-384.
13. Liu, M.T. Dexheimer D. Sui S. Hovde X. Deng R. Kwok D.A. Bochar M.-H.J.S.r. Kuo, *Hyperphosphorylated tau aggregation and cytotoxicity modulators screen identified prescription drugs linked to Alzheimer's disease and cognitive functions*. 2020. **10**(1): p. 1-14.
14. Ballatore, C.V.M.-Y. Lee J.Q.J.N.r.n. Trojanowski, *Tau-mediated neurodegeneration in Alzheimer's disease and related disorders*. 2007. **8**(9): p. 663-672.
15. Martin, L.X. Latypova C.M. Wilson A. Magnaudeix M.L. Perrin C. Yardin F. Terro, *Tau protein kinases: Involvement in Alzheimer's disease*. Ageing Research Reviews, 2013. **12**(1): p. 289-309.
16. Liu, F.K. Iqbal. Grundke-Iqbal C.-X.J.F.I. Gong, *Involvement of aberrant glycosylation in phosphorylation of tau by cdk5 and GSK-3 $\beta$* . 2002. **530**(1-3): p. 209-214.
17. Tian, Z.H. Yu L. Wang M. Saleem F. Ren P. Ren Y. Chen R. Sun Y. Sun L. Huang, *Recent progress in the preparation of polyaniline nanostructures and their applications in anticorrosive coatings*. RSC Advances, 2014. **4**(54).
18. Kaneto, K.M. Kaneko Y. Min A.G. MacDiarmid, *Artificial muscle : Electromechanical actuators using polyaniline films*. Synthetic Metals 1995. **71**(1-3): p. 2211-2212.

19. Ćirić-Marjanović, G., *Recent advances in polyaniline research: Polymerization mechanisms, structural aspects, properties and applications*. Synthetic Metals, 2013. **177**: p. 1-47.
20. Boeva, Z.A.V.G. Sergeev, *Polyaniline: Synthesis, properties, and application*. Polymer Science Series C, 2014. **56**(1): p. 144-153.
21. Wang, G.W. WuH. YangP. ZhangJ.Y. Wang, *Intact polyaniline coating as a conductive guidance is beneficial to repairing sciatic nerve injury*. Journal of Biomedical Materials Research Part B : Applied Biomaterials, 2020. **108**(1): p. 128-142.
22. Fan, L.Y. XiongZ. FuD. XuL. WangY. ChenH. XiaN. PengS. YeY. WangL. ZhangQ. Ye, *Polyaniline promotes peripheral nerve regeneration by enhancement of the brain-derived neurotrophic factor and ciliary neurotrophic factor expression and activation of the ERK1/2/MAPK signaling pathway*. Molecular Medicine Reports, 2017. **16**(5): p. 7534-7540.
23. Van De Pol, L.A.A. HenselW.M. van der FlierP.J. VisserY.A. PijnenburgF. BarkhofH.J. GertzP.J.J.o.N. Scheltens, *NeurosurgeryPsychiatry, Hippocampal atrophy on MRI in frontotemporal lobar degeneration and Alzheimer's disease*. 2006. **77**(4): p. 439-442.
24. Hashimoto, M.H. KazuiK. MatsumotoY. NakanoM. YasudaE.J.A.J.o.P. Mori, *Does donepezil treatment slow the progression of hippocampal atrophy in patients with Alzheimer's disease?* 2005. **162**(4): p. 676-682.
25. Huang, L.J. HuL. LangX. WangP. ZhangX. JingX. WangX. ChenP.I. LelkesA.G.J.B. MacDiarmid, *Synthesis and characterization of electroactive and biodegradable ABA block copolymer of polylactide and aniline pentamer*. 2007. **28**(10): p. 1741-1751.
26. Tainaka, K.M. InoueA. HirataT. MoriiT. Konno, *Charge-Pairing Mechanism of Phosphorylation Effect upon Amyloid Fibrillation of Human Tau Core Peptide*. Biochemistry, 2008. **47**: p. 11847–11857.
27. Dolan, P.J.G.V. Johnson, *The role of tau kinases in Alzheimer's disease*. Current Opinion in Drug Discovery & Development, 2010. **12**(5): p. 595–603.
28. Astuti, Y.E. TopoglidisG. GilardiJ.R. Durrant, *Cyclic voltammetry and voltabsorptometry studies of redox proteins immobilised on nanocrystalline tin dioxide electrodes*. Bioelectrochemistry, 2004. **63**(1-2): p. 55-9.
29. Hayes, M.A.E.W. KristensenW.G. Kuhr, *Background-subtraction of fast-scan cyclic staircase voltammetry at protein-modified carbon-fiber electrodes*. Biosensors and Bioelectronics, 1998. **13**: p. 1297–1305.
30. Wilm, M.G. NeubauerM. Mann, *Parent Ion Scans of Unseparated Peptide Mixtures*. Analytical Chemistry, 1996. **68**: p. 527-533.
31. Schlosser, A.R. PipkornD. BossemeyerW.D. Lehmann, *Analysis of Protein Phosphorylation by a Combination of Elastase Digestion and Neutral Loss Tandem Mass Spectrometry*. Analytical Chemistry, 2001. **73**: p. 170-176.
32. Sun, Y.J. HuangY. ChenH. ShangW. ZhangJ. YuL. HeC. XingC. Zhuang, *Direct inhibition of Keap1-Nrf2 Protein-Protein interaction as a potential therapeutic strategy for Alzheimer's disease*. Bioorganic Chemistry, 2020. **103**: p. 104172.

33. Hensley, K.M.L. MaidtZ. YuH. SangR.A. Floyd, *Electrochemical Analysis of Protein Nitrotyrosine and Dityrosine in the Alzheimer Brain Indicates Region-Specific Accumulation*. The Journal of Neuroscience, 1998. **18**(20): p. 8126–8132.
34. Jahnke, H.G.A. BraesigkT.G. MackS. PonickF. StriggowA.A. Robitzki, *Impedance spectroscopy based measurement system for quantitative and label-free real-time monitoring of tauopathy in hippocampal slice cultures*. Biosensors and Bioelectronics, 2012. **32**(1): p. 250-8.
35. Shumyantseva, V.V.E.V. SuprunT.V. BulkoA.I. Archakov, *Electrochemical methods for detection of post-translational modifications of proteins*. Biosensors and Bioelectronics, 2014. **61**: p. 131-9.
36. Ge, X.A. ZhangY. LinD. Du, *Simultaneous immunoassay of phosphorylated proteins based on apoferritin templated metallic phosphates as voltammetrically distinguishable signal reporters*. Biosensors and Bioelectronics, 2016. **80**: p. 201-207.
37. Miao, P.L. NingX. LiP. LiG. Li, *Electrochemical strategy for sensing protein phosphorylation*. Bioconjugate Chemistry, 2012. **23**(1): p. 141-145.
38. Amit, E.R. ObenaY.T. WangR. ZhuravelA.J.F. ReyesS. ElbazD. RotemD. PorathA. FriedlerY.J. ChenS. Yitzchaik, *Integrating proteomics with electrochemistry for identifying kinase biomarkers*. Chemical Science, 2015. **6**(8): p. 4756-4766.
39. Sbei, N.G.M. MartinsB. ShirinfarN. Ahmed, *Electrochemical Phosphorylation of Organic Molecules*. Chemical Record, 2020. **20**: p. 1-24.
40. Jahnke, H.G.D. KrinkeD. SeidelK. LilienthalS. SchmidtR. AzendorfM. FischerT. MackF. StriggowH. AlthausA. SchoberA.A. Robitzki, *A novel 384-multiwell microelectrode array for the impedimetric monitoring of Tau protein induced neurodegenerative processes*. Biosensors and Bioelectronics, 2017. **88**: p. 78-84.
41. Wang, S.X.D. AchaA.J. ShahF. Hillsl. RoittA. DemosthenousR.H. Bayford, *Detection of the tau protein in human serum by a sensitive four-electrode electrochemical biosensor*. Biosensors and Bioelectronics, 2017. **92**: p. 482-488.
42. Martić, S.S. BeheshtiH.-B. Kraatz, *Electrochemical Investigations of Tau Protein Phosphorylations and Interactions with Pin1*. Chemistry & Biodiversity, 2012. **9**.
43. Martić, S.S. BeheshtiM.K. RainsH.B. Kraatz, *Electrochemical investigations into Tau protein phosphorylations*. Analyst, 2012. **137**(9): p. 2042-6.
44. Sakai, K.Y. SugimotoY. KitazumiO. ShiraiK. TakagiK. Kano, *Direct electron transfer-type bioelectrocatalytic interconversion of carbon dioxide/formate and NAD<sup>+</sup>/NADH redox couples with tungsten-containing formate dehydrogenase*. Electrochimica Acta, 2017. **228**: p. 537-544.
45. Thoi, V.S.H.I. KarunadasaY. SurendranathJ.R. LongC.J. Chang, *Electrochemical generation of hydrogen from acetic acid using a molecular molybdenum–oxo catalyst*. Energy & Environmental Science, 2012. **5**(7).
46. Dargahi, M.E. KonkovS. Omanovic, *Influence of Surface Charge/Potential of a Gold Electrode on the Adsorptive/Desorptive Behaviour of Fibrinogen*. Electrochimica Acta, 2015. **174**: p. 1009-1016.

# Figures

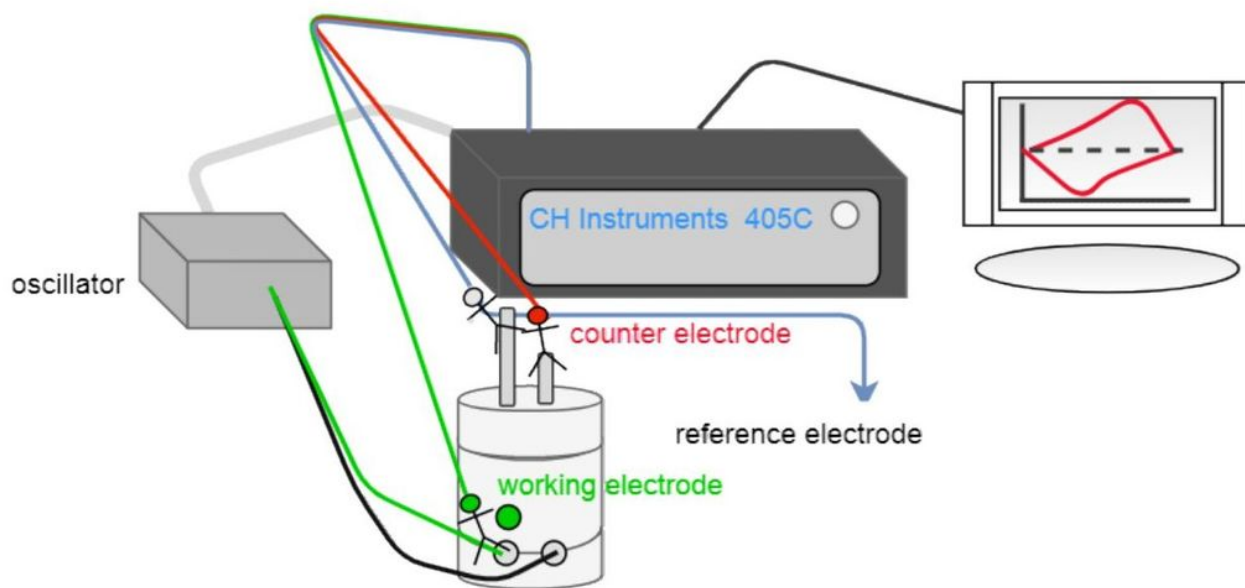
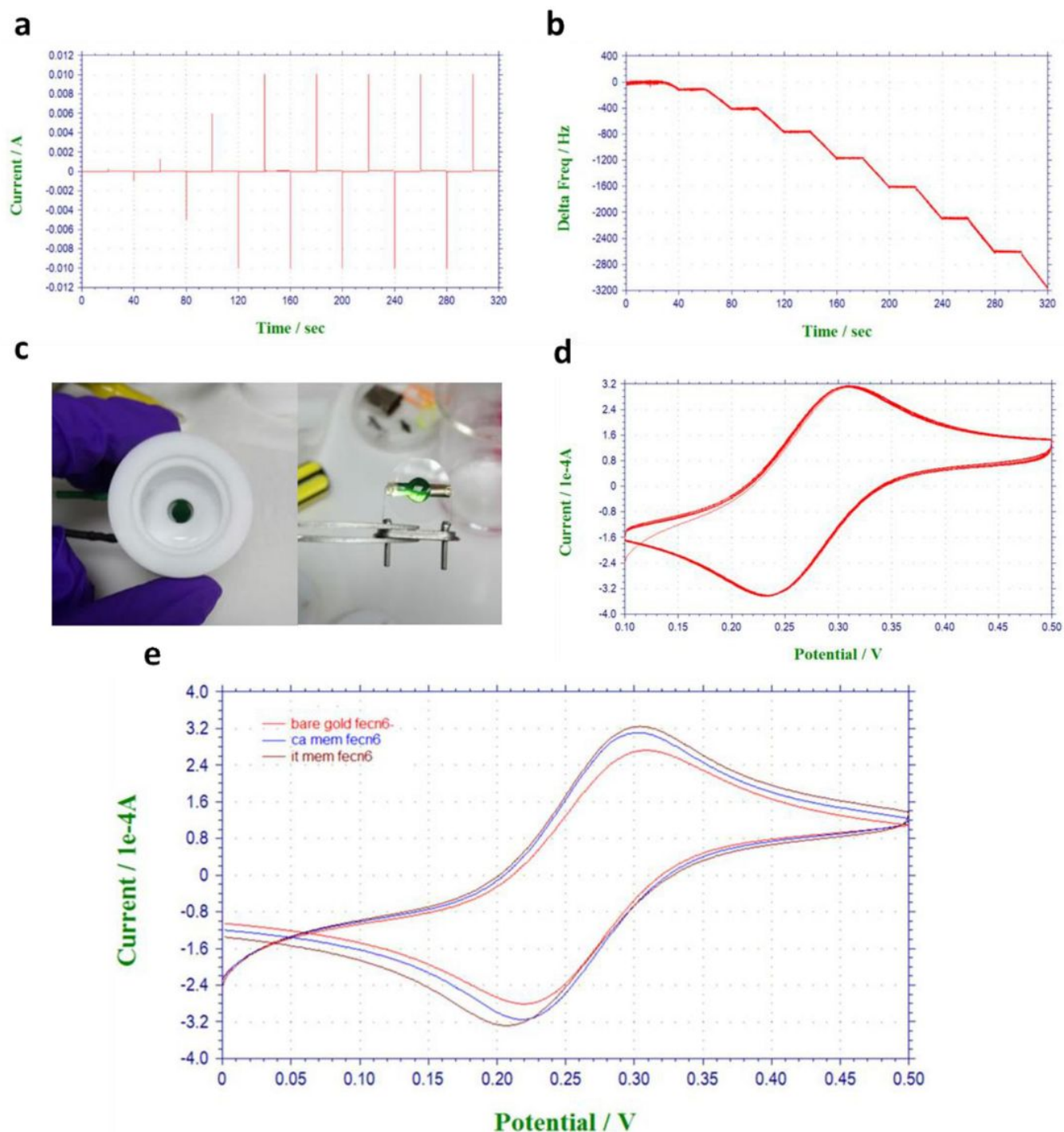


Figure 1

Schematic diagram of electrochemical analysis device



**Figure 2**

Using chronoamperometry to generate a polyaniline film on the electrode (a) A plot showing current versus time dynamics while using chronoamperometry to make a polyaniline film on the electrode, (b) A plot showing delta frequency versus time dynamics while using chronoamperometry to make a polyaniline film on the electrode, (c) Image of PANI film formed by chronoamperometric polymerization of aniline (d) Cyclic voltammetry 0.1 V to 0.5 V fifty times inside  $\text{Fe}(\text{CN})_6^{4-} / \text{Fe}(\text{CN})_6^{3-}$  solution to test the conductivity of the PANI membrane made by chronoamperometry (e) Comparison of Cyclic Voltammetry sweep in  $\text{Fe}(\text{CN})_6^{4-} / \text{Fe}(\text{CN})_6^{3-}$  solution after different PANI films were attached and bare gold electrode.

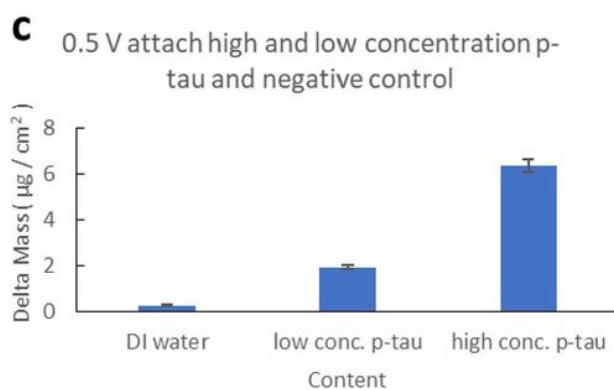
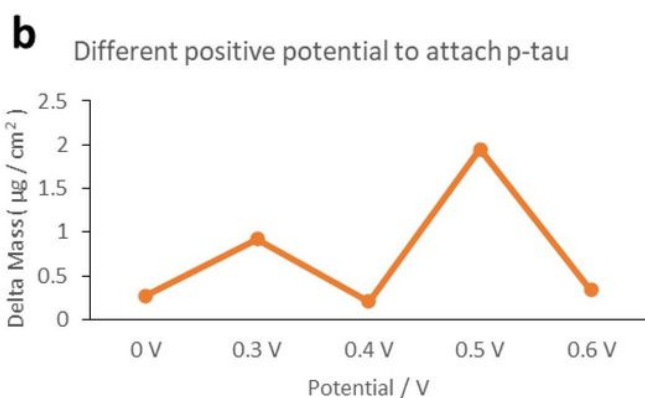
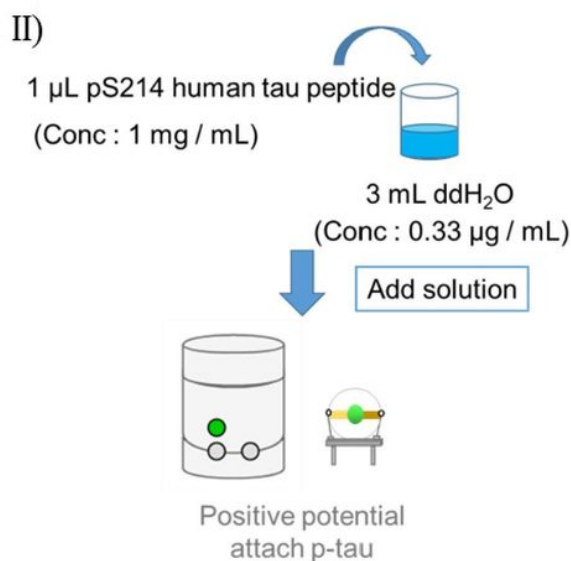
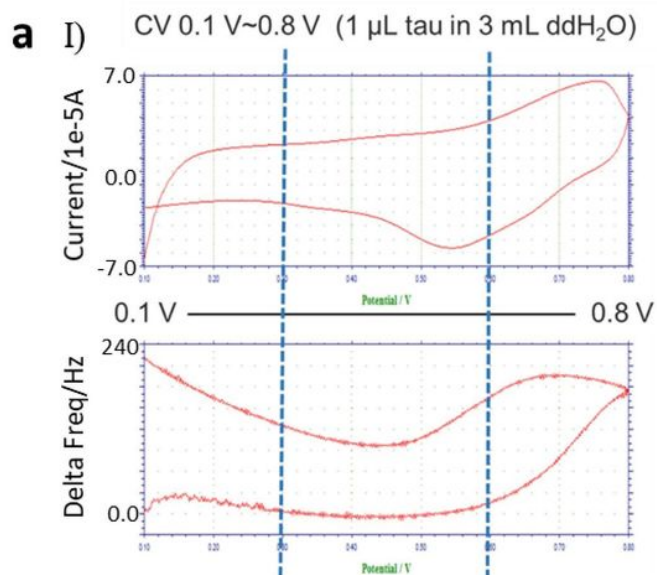


**Figure 3**

Using positive potential to attach p-tau (a) Cyclic voltammetry to filter positive potential. I) Cyclic voltammetry swept the positive potential window from 0.1 V to 0.8 V. II) The protocol of solution change in the cell (b) Using different positive potential to attach p-tau (c) Using 0.5 V to attach different concentration p-tau solution

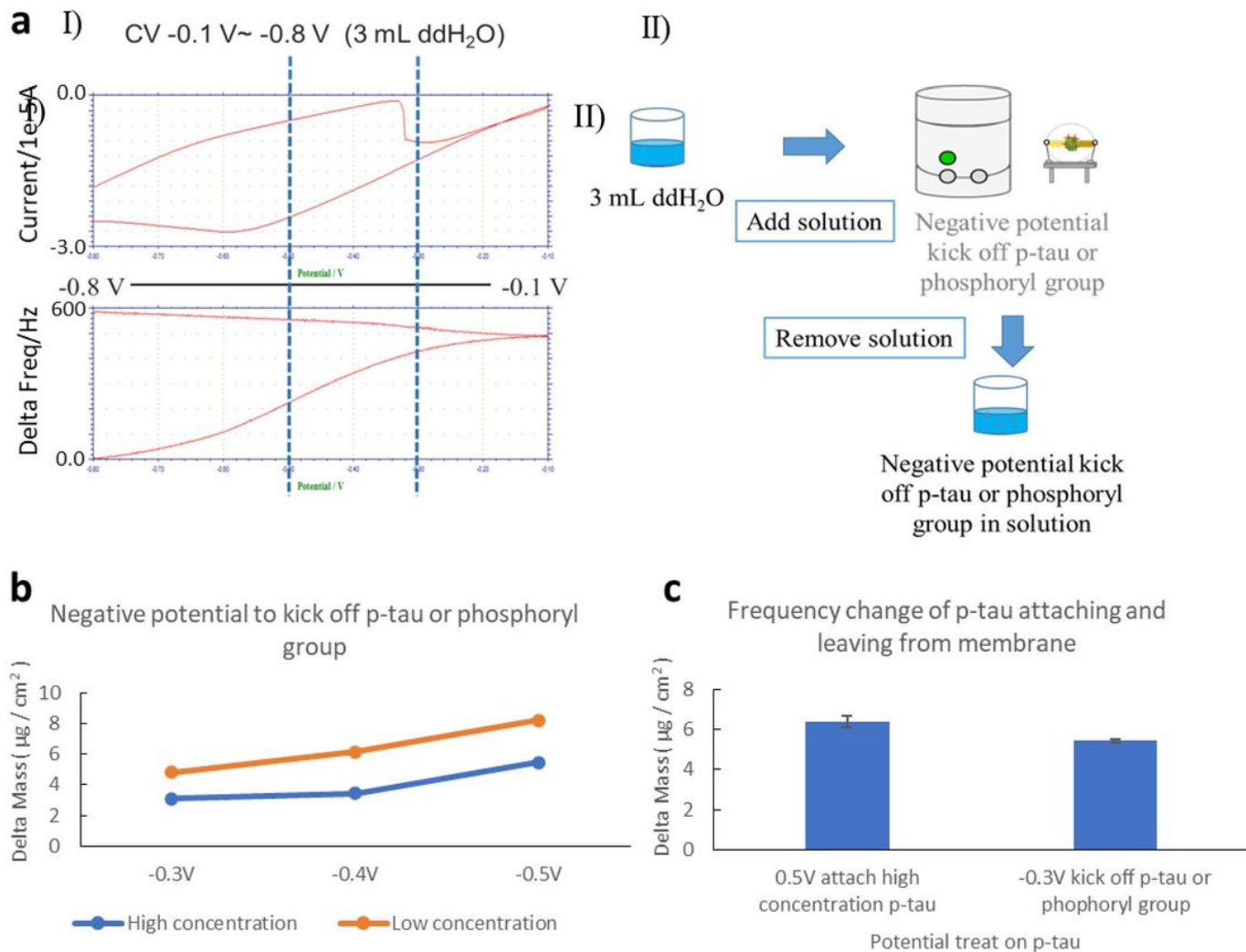


**Figure 4**

Fixed negative potential was used to dephosphorylate p-tau (a) Cyclic voltammetry to filter negative potential. I) Cyclic voltammetry sweep for the negative potential range from -0.8 V to -0.1 V. II) The protocol for solution change in the cell (b) Negative potential to remove p-tau or phosphoryl group (High concentration and low concentration) (c) Frequency change on the electrode due to p-tau attaching and leaving from membrane

